ANALYTICAL ANALYSIS FOR SPACE FRACTIONAL HELMHOLTZ EQUATIONS BY USING THE HYBRID EFFICIENT APPROACH

Adnan KHAN*/**⬤**, Muhammad Imran LIAQAT*/****⬤**, Asma MUSHTAQ****⬤

*National College of Business Administration & Economics, Lahore, Pakistan
**Abdus Salam School of Mathematical Sciences, Government College University, 68-B,
New MuslimTown, Lahore 54600, Pakistan

adnankhantariq@ncbae.edu.pk, imran_liaqat_22@sms.edu.pk, Asmafaizan624@gmail.com

Abstract: The Helmholtz equation is an important differential equation. It has a wide range of uses in physics, including acoustics, electrostatics, optics, and quantum mechanics. In this article, a hybrid approach called the Shehu transform decomposition method (STDM) is implemented to solve space-fractional-order Helmholtz equations with initial boundary conditions. The fractional-order derivative is regarded in the Caputo sense. The solutions are provided as series, and then we use the Mittag-Leffler function to identify the exact solutions to the Helmholtz equations. The accuracy of the considered problem is examined graphically and numerically by the absolute, relative, and recurrence errors of the three problems. For different values of fractional-order derivatives, graphs are also developed. The results show that our approach can be a suitable alternative to the approximate methods that exist in the literature to solve fractional differential equations.

Key words: Helmholtz equations, Shehu transform, Adomian decomposition method, Mittag-Leffler function, Caputo derivatives

1. INTRODUCTION

The fractional calculus (FC) results from several straightforward questions regarding the concept of derivatives: why does a function's half-order derivative reveal information that the first-order derivative does not? By providing answers to these issues, researchers create a new window of opportunity between the mathematical and physical worlds, leading to several exciting new questions and findings. For instance, unlike the conventional derivative, the fractional-order derivative (FOD) of a constant function is not always zero [1].

The memory idea is the most beneficial interpretation of FC. In general, systems are considered to be memoryless when their output at each time t depends only on the input at time t. However, when the system has to remember past values of the input to compute the present value of the output, these systems are referred to as memory systems or non-memoryless systems. The memory property of FOD refers to their ability to capture and incorporate information from past states. Instead of traditional integer-order derivatives, which rely solely on the current state of a system, FOD retain memory of past states over a certain time horizon. This memory property is particularly useful in modeling and analyzing systems with long-term dependencies or non-local effects, where past events continue to influence the system's dynamics alongside the current state. By incorporating information from past states, FOD provide a more accurate representation of the system's behavior and enable better predictions of its future evolution. In practical terms, the memory property of FOD allows for a more nuanced understanding of complex phenomena in various fields, including physics, engineering, biology, finance, and more. It facilitates the development of more accurate models and control strategies for systems exhibiting non-local or long-term memory effects.

Different from integer-order derivatives, there are several kinds of definitions for FOD [2-5]. These definitions are generally not equivalent to each other. In the following, we introduce several definitions.

The natural derivative is fundamentally extended into a fractional derivative by the Grünwald-Letnikov derivative. Both Anton Karl Grünwald and Aleksey Vasilievich Letnikov introduced it in 1867 and 1868, respectively [6]. It is therefore written as:

$$\Im^\varsigma \varXi(\tau) = \lim_{\hbar \to 0} \frac{1}{\hbar} \sum_{\kappa=0}^{\infty} (-1)^\kappa \begin{bmatrix} \varsigma \\ \kappa \end{bmatrix} \varXi(\tau - \kappa\hbar),$$

where $\kappa \in N$, and the gamma function is used to determine the binomial coefficient,

$$\begin{bmatrix} \varsigma \\ \kappa \end{bmatrix} = \frac{\varsigma(\varsigma-1)(\varsigma-2)(\varsigma-3)\cdots(\varsigma-\kappa+1)}{\kappa!}.$$

In 1847, Riemann defined the new fractional order derivative that is called Riemann-Liouville fractional derivatives (RLFD) [7]. It is defined as follows:

$$\Im_{0,\tau}^\varsigma \varXi(\tau) = \frac{d^\kappa}{d\tau^\kappa} D_{0,\tau}^{-(\kappa-\varsigma)} \varXi(\tau) = \frac{1}{\Gamma(\kappa-\varsigma)} \frac{d^\kappa}{d\tau^\kappa} \int_0^\tau (\tau - \varUpsilon)^{\kappa-\varsigma-1} \varXi(\varUpsilon) d\varUpsilon,$$

where $\kappa - 1 \le \varsigma < \kappa \in Z^+$

The Caputo fractional derivative (CFD) was established in 1967 [8] because it was ineffective in the description and modelling of some complicated events.

$$\Im_{0,\tau}^\varsigma \varXi(\tau) = D_{0,\tau}^{-(\kappa-\varsigma)} \frac{d^\kappa}{d\tau^\kappa} \varXi(\tau) = \frac{1}{\Gamma(\kappa-\varsigma)} \int_0^\tau (\tau - \varUpsilon)^{\kappa-\varsigma-1} \frac{d^\kappa}{d\tau^\kappa} \varXi(\varUpsilon) d\varUpsilon,$$

where $\kappa - 1 \le \varsigma < \kappa \in Z^+$

The RLFD of a constant W is given by $\frac{W\tau^{-\kappa}}{\Gamma(1-\varsigma)}$. As a result, the CFD's ability to provide the derivative of a constant zero, as in an ordinary derivative, is one of its strengths.

It is important to keep in mind that while all FOD behave the same when the order is an integer, they may behave differently when the order is not an integer. For instance, in a non-integer order, the CFD of a constant behaves differently than the RLFD because it is zero. There are more fractional derivatives; the interested reader is referred to [9-12] for further details.

Fractional-order differential equations (FODEs) are mathematical representations of natural and physical phenomena that occur in the fields of science and engineering. As a result, we detect the mechanism of these FODEs through the study of the approximate and exact solution, and their genuine physical intention can be understood from the graphical representation of the solution.

Due to their arbitrary features, FODEs are thought to be more difficult to compute than integer-order differential equations. In the literature, several methods are developed over the past few decades, namely the invariant subspace method [13], the Lie symmetry approach [14], the (G/G)-Expansion Method [15], the Haar wavelet method [16], the operational matrix method [17], and the sub-equation method [18] to solve the fractional differential and integral equations.

However, in some circumstances, especially when dealing with large and complex problems, the approximate solution technique for handling FODEs proves to be more effective and practical. As a result, different approximate techniques are created by researchers to solve various types of FODEs. For instance, the operational matrix approach [19], the Elzaki residual power series approach [20], the homotopy analysis method [21], and the decomposition method [22], for more approximate techniques, see [23-25]. Absolute, relative, and recurrence errors are commonly used to assess the accuracy of approximate methods in solving mathematical problems. By analyzing these error measures, researchers can gain a comprehensive understanding of the performance of approximate methods. Indeed, most researchers commonly utilize absolute, relative, and recurrence errors as primary metrics for assessing the accuracy and convergence of approximate methods in solving mathematical problems [26-29].

The wave equation can be used to derive the Helmholtz equation (HH-E), an elliptic partial differential equation. The HH-E is used to explain a variety of phenomena, including electromagnetic waves in fluids, vibrating lines, plates, and walls, as well as acoustics, magnetic fields, nuclear power plants, and geoscience. Take into account a 2D non-homogeneous isotropic material whose Euclidean space velocity is V. The wave result, $\Xi(\nu, \varpi)$, which has the harmonic origin $\Theta(\nu, \varpi)$ as its point of vibration and vibrates at the fixed frequency $\omega > 0$, satisfies the HH-E for the defined area R.

$$\frac{\partial^2}{\partial \nu^2}\Xi(\nu, \varpi) + \frac{\partial^2}{\partial \varpi^2}\Xi(\nu, \varpi) + \Omega\Xi(\nu, \varpi) = -\Theta(\nu, \varpi),$$

where $\Xi(\nu, \varpi)$ is an appropriately differentiable function at the boundary of R, and $\Theta(\nu, \varpi)$ is a specified function, $\Omega > 0$ is a constant value, and $\sqrt{\Omega} = \frac{\omega}{V}$ is a wave number with a wavelength of $\frac{2\pi}{\sqrt{\Omega}}$.

In this research, STDM is applied to the HH-E in the sense of CFD of x-space in the following form:

$$\Im_\nu^\varsigma \Xi(\nu, \varpi) + \frac{\partial^2}{\partial \varpi^2}\Xi(\nu, \varpi) + \Omega\Xi(\nu, \varpi) = -\Theta(\nu, \varpi),\ 1 < \varsigma \leq 2,$$

subject to the initial conditions (I-Cs)

$$\Xi(\nu, 0) = \Psi(\varpi), \Xi_\nu(\nu, 0) = T(\varpi).$$

Furthermore, we similarly apply STDM to the HH-E in terms of the CFD of y-space:

$$\Im_\varpi^\varsigma \Xi(\nu, \varpi) + \frac{\partial^2}{\partial \nu^2}\Xi(\nu, \varpi) + \Omega\Xi(\nu, \varpi) = -\Theta(\nu, \varpi),\ 1 < \varsigma \leq 2.$$

with the following I-Cs:

$$\Xi(\nu, 0) = \Phi(\nu), \Xi_\varpi(\nu, 0) = P(\nu).$$

In general, boundary conditions for the HH-E specify the behavior of the solution at the boundaries of the domain in which the equation is being solved. These boundary conditions can be of various types, including Dirichlet boundary conditions, Neumann boundary conditions, or mixed boundary conditions.

Dirichlet boundary conditions: These specify the value of the solution at the boundary of the domain. Mathematically, it can be expressed as $\Xi(\nu, \varpi) = g(\nu, \varpi)$, where $g(\nu, \varpi)$ is a given function describing the boundary values.

Neumann boundary conditions: These specify the normal derivative of the solution at the boundary of the domain. Mathematically, it can be expressed as

$$\frac{\partial}{\partial n}\Xi(\nu, \varpi) = f(\nu, \varpi),$$

where $f(\nu, \varpi)$ is a given function describing the normal derivative on the boundary.

Mixed boundary conditions: These are a combination of Dirichlet and Neumann boundary conditions, specifying both the value of the solution and its normal derivative at different parts of the boundary.

The choice of boundary conditions depends on the physical problem and the geometry of the domain. For example, in acoustic problems, Dirichlet boundary conditions might be used to specify the pressure at the boundaries of a room, while in electromagnetic problems, Neumann boundary conditions might be used to specify the normal component of the electric field at a conducting boundary.

The solution of the HH-E holds significant importance across various fields of science and engineering due to its wide range of applications. Here are some reasons highlighting its importance:

Acoustics: In acoustics, the HH-E describes the behavior of sound waves in different media. Solutions to this equation help in understanding phenomena such as sound propagation, resonance, and wave interference. Applications include designing concert halls, noise control, and ultrasound imaging.

Electromagnetics: In electromagnetics, the HH-E describes the behavior of electromagnetic fields, such as those produced by antennas, waveguides, and resonant cavities. Solutions to this equation are crucial for designing communication systems, radar systems, and microwave devices.

Optics: In optics, the HH-E governs the propagation of light waves through various optical media. Solutions to this equation are essential for designing optical components, such as lenses, mirrors, and optical fibers, as well as for understanding phenomena like diffraction and interference.

Quantum mechanics: In quantum mechanics, the HH-E appears in the context of the Schrödinger equation, which describes the behavior of quantum particles in potential fields. Solutions to this equation provide insights into the energy levels and wave functions of quantum systems, with applications in atomic physics, solid-state physics, and quantum chemistry.

Adnan Khan, Muhammad Imran Liaqat, Asma Mushtaq
Analytical Analysis for Space Fractional Helmholtz Equations by using the Hybrid Efficient Approach

DOI 10.2478/ama-2024-0065

Engineering: In general engineering applications, the HH-E arises in problems involving wave propagation, vibration analysis, and structural dynamics. Solutions to this equation are essential for designing structures, predicting their response to external forces, and optimizing their performance.

Overall, the solution of the HH-E plays a crucial role in understanding and modeling various physical phenomena, enabling the development of innovative technologies and solutions across different fields.

One of the most helpful mathematical methods is the use of integral transforms to solve differential equations (DEs) and integral equations. DEs can be expressed in terms of a straightforward algebraic equation by selecting the appropriate integral transform (IT). Many mathematicians are interested in a novel IT known as the "Shehu transforms (Sh-T)". The suggested IT is effectively applied to both ordinary and partial DEs, and it is derived from the classical Fourier IT.

In this paper, the HH-E problem is solved in the context of CFD using the Sheu transform (Sh-T) and the Adomian decomposition method (ADM). The primary advantage of this method is that it does not call for the solution of any parameters in the equation. Consequently, it circumvents certain limitations associated with traditional perturbation techniques. The accuracy and effectiveness of the STDM are confirmed by comparing the approximate solution (App-S) and the exact solution (Ex-S). Additionally, 2D graphs are generated for various values of FOD, illustrating the convergence of the approximation solution to the Ex-S as FOD increases. Therefore, results show that the fifth-step App-S perfectly agrees with the exact solution. The numerical analysis in the sense of absolute errors (Abs-Er), relative errors (Rel-Er), and recurrence errors (Rec-Er) evaluations establish the correctness and convergence, proving the effectiveness of the suggested method. Therefore, our suggested approach is effective and simple to apply to many different kinds of related scientific and technical problems.

The major contributions of this paper include at least the following aspects: The system we study is more generalized because it includes the FOD. For the first time in literature, we use the Shehu transform to solve fractional Helmholtz equations. We obtain both approximate and exact solutions. The suggested approach is a useful tool for both exact and approximate FODE solutions. The strength of the scheme lies in the modest size of computation required for the proposed approach, which yields accuracy with fewer computations. The efficiency and reliability of the recommended approach are demonstrated by the error analysis.

The following is how this study is structured: First, in Section 2, we use key definitions and findings from FC theory. The algorithm STDM for solving space-fractional Helmholtz equations is then covered in Section 3. Some problems in Section 4 are solved with the use of STDM. In Section 5, we also present a graphic and numerical comparison of approximate and exact solutions in terms of Abs-Er, Rel-Er, and Rec-Er, demonstrating the validity of the suggested approach. Lastly, we provide a summary of our findings in the conclusion.

2. PRELIMINARY CONCEPTS

We provide some helpful definitions related to FC in this section. The Mittag-Leffler function (ML-F), which is important in FC,

is defined first. Next, we go through some fundamental Sh-T terms, definitions, and theorems that are relevant to this study.

Definition 1. [30] A direct generalization of the exponential function, e^v, is the ML-F. The power series formula for the two-parameter ML-F is as follows:

$$E_{\alpha,\beta}(v) = \sum_{\kappa=0}^{\infty} \frac{v^\kappa}{\Gamma(\alpha\kappa+\beta)}, \alpha > 0, \beta > 0.$$

The definition of the one-parameter ML-F is:

$$E_\alpha(v) = \sum_{\kappa=0}^{\infty} \frac{v^\kappa}{\Gamma(\alpha\kappa+1)}, \alpha > 0.$$

We get well-known classical functions when the parameters α, β are chosen in specific ways.

$$E_{1,1}(v) = e^v, E_{1,2}(v) = \frac{e^v-1}{v}, E_{2,1}(v^2) = \cosh v, E_{2,2}(v^2) = \frac{\sinh v}{v}.$$

Definition 2. [31] The Sh-T is defined as follows:
$$S[\Xi(v,\varpi)] = P(\mu,\eta) = \int_0^\infty \Xi(v,\varpi)e^{\frac{-\mu v}{\eta}} dv, v > 0,$$

The inverse Sh-T is given by

$$S^{-1}\{P(\mu,\eta)\} = \Xi(v,\varpi) = \frac{1}{2\pi i}\int_{w-i\infty}^{w+i\infty} \frac{1}{v}P(\mu,\eta)e^{\frac{-\mu v}{\eta}} d\mu,$$

where μ and η are the Sh-T variables, and w is a real constant, and the integral is taken along $\mu = w$ in the complex plane $s = v + \varpi i$.

Some important properties of Sh-T are as follows [32]

$$S[\Lambda_1 \Xi_1(v) + \Lambda_2 \Xi_2(v)] = \Lambda_1 S[\Xi_1(v)] + \Lambda_2 S[\Xi_2(v)].$$

$$S[1] = \frac{\mu}{\eta}.$$

$$S\left[\frac{v^n}{n!}\right] = \left(\frac{\mu}{\eta}\right)^{n+1} \text{ for } n = 0,1,2,3,\ldots$$

$$S[v^\varsigma] = \left(\frac{\mu}{\eta}\right)^{\varsigma+1} \Gamma(\varsigma+1).$$

Definition 3. [32] The Sh-T for nth derivatives is defined as

$$S[\mathfrak{F}^{(n)}\Xi(v)] = \frac{\mu^n}{\eta^n}S[\Xi(v)] - \sum_{\kappa=0}^{n-1}\left(\frac{\mu}{\eta}\right)^{n-\kappa-1} \Xi^{(\kappa)}(0), n \geq 1.$$

Definition 4. [33] The Sh-T of CFD of $\Xi(v,\varpi)$ with order ς is defined as

$$S[\mathfrak{F}^{(\varsigma)}\Xi(v)] = \frac{\mu^\varsigma}{\eta^\varsigma}S[\Xi(v)] -$$
$$\sum_{\kappa=0}^{\kappa-1}\left(\frac{\mu}{\eta}\right)^{\varsigma-\kappa-1} \Xi^{(\kappa)}(0), \kappa-1<\varsigma < \kappa.$$

3. ALGORITHM OF THE SHEHU TRANSFORM DECOMPOSITION METHOD

The primary goal of this section is to provide a series-form solution for the HH-E using STDM. The main algorithms of STDM are as follows: To do so, first apply the Sh-T to both sides of the given problem to convert the given model into algebraic expressions, and then use the inverse Sh-T to convert the obtained algebraic expression into the model's real domain. In the next step, we provide the series solutions of the model by using the ADM on the algebraic expressions that are attained with the help of Sh-T and inverse Sh-T.

As the fundamental idea of the suggested technique, we take into consideration a general form of HH-E:

$$\frac{\partial^2}{\partial v^2}\Xi(v,\varpi) + \frac{\partial^2}{\partial \varpi^2}\Xi(v,\varpi) + \Omega\Xi(v,\varpi) = -\Theta(v,\varpi), \quad (1)$$

with the I-Cs

$$\Xi(0,\varpi) = \Phi(\varpi), \Xi_v(0,\varpi) = P(\varpi). \quad (2)$$

Applying the Sh-T to Eq. (1), we use the differentiation property of the Sh-T, and after some calculation, as a result, we get as follows:

$$S[\Xi(v,\varpi)] = \frac{\eta}{\mu}\Phi(\varpi) - \left(\frac{\eta}{\mu}\right)^\varsigma S[\frac{\partial^2}{\partial\varpi^2}\Xi(v,\varpi)] -$$
$$\left(\frac{\eta}{\mu}\right)^\varsigma \Omega S[\frac{\partial^2}{\partial\lambda^2}\Xi(v,\varpi)] - \left(\frac{\eta}{\mu}\right)^\varsigma S[\Theta(v,\varpi)], \quad (3)$$

Taking the inverse Sh-T on Eq. (2), we have

$$\Xi(v,\varpi) = S^{-1}[\frac{\eta}{\mu}\Phi(\varpi)] - S^{-1}[\left(\frac{\eta}{\mu}\right)^\varsigma S[\frac{\partial^2}{\partial\varpi^2}\Xi(v,\varpi)]] -$$
$$S^{-1}[\left(\frac{\eta}{\mu}\right)^\varsigma \Omega S[\frac{\partial^2}{\partial\lambda^2}\Xi(v,\varpi)]] - S^{-1}[\left(\frac{\eta}{\mu}\right)^\varsigma S[\Theta(v,\varpi)]], \quad (4)$$

Implementing ADM in Eq. (4), therefore, supposes that the solution of Eq. (1) can be expressed as follows:

$$\Xi(v,\varpi) = \sum_{\kappa=0}^{\infty}\Xi_\kappa(v,\varpi). \quad (5)$$

Using Eq. (5) in Eq. (4).

$$\Xi(v,\varpi) = S^{-1}[\frac{\eta}{\mu}\Phi(\varpi)] -$$
$$S^{-1}[\left(\frac{\eta}{\mu}\right)^\varsigma S[\frac{\partial^2}{\partial\varpi^2}\sum_{\kappa=0}^{\infty}\Xi_\kappa(v,\varpi)]] -$$
$$S^{-1}[\left(\frac{\eta}{\mu}\right)^\varsigma \Omega S[\frac{\partial^2}{\partial\lambda^2}\sum_{\kappa=0}^{\infty}\Xi_\kappa(v,\varpi)]] - S^{-1}[\left(\frac{\eta}{\mu}\right)^\varsigma S[\Theta(v,\varpi)]]. \quad (6)$$

By comparing the two sides of Eq. (6), we arrive at the following terms for the series solution:

$$\Xi_0(v,\varpi) = S^{-1}[\frac{\eta}{\mu}\Phi(\varpi)] - S^{-1}[\left(\frac{\eta}{\mu}\right)^\varsigma S[\Theta(v,\varpi)]].$$

$$\Xi_1(v,\varpi) = -S^{-1}[\left(\frac{\eta}{\mu}\right)^\varsigma S[\frac{\partial^2}{\partial\varpi^2}\Xi_0(v,\varpi)]] -$$
$$S^{-1}[\left(\frac{\eta}{\mu}\right)^\varsigma \Omega S[\frac{\partial^2}{\partial\lambda^2}\Xi_0(v,\varpi)]].$$

$$\Xi_2(v,\varpi) = -S^{-1}[\left(\frac{\eta}{\mu}\right)^\varsigma S[\frac{\partial^2}{\partial\varpi^2}\Xi_1(v,\varpi)]] -$$
$$S^{-1}[\left(\frac{\eta}{\mu}\right)^\varsigma \Omega S[\frac{\partial^2}{\partial\lambda^2}\Xi_1(v,\varpi)]].$$

$$\Xi_{\kappa+1}(v,\varpi) = -S^{-1}[\left(\frac{\eta}{\mu}\right)^\varsigma S[\frac{\partial^2}{\partial\varpi^2}\Xi_\kappa(v,\varpi)]] -$$
$$S^{-1}[\left(\frac{\eta}{\mu}\right)^\varsigma \Omega S[\frac{\partial^2}{\partial\lambda^2}\Xi_\kappa(v,\varpi)]].$$

We can quickly reach the convergent series because it is simple to determine the $\Xi(v,\varpi)$ component. We can acquire as $\kappa \to \infty$.

$$\Xi(v,\varpi) = \lim_{\kappa\to\infty}\Xi_\kappa(v,\varpi).$$

4. NUMERICAL EXAMPLES

To comprehend the steps of the suggested approach, we apply the STDM to three problems in this section of the paper.

Example 3.1 Consider the v-space fractional-order HH-E.

$$\mathfrak{I}_v^\varsigma\Xi(v,\varpi) + \frac{\partial^2}{\partial\varpi^2}\Xi(v,\varpi) - \Xi(v,\varpi) = 0, 1<\varsigma \le 2, \quad (7)$$

with the I-Cs

$$\Xi(0,\varpi) = \varpi, \Xi_v(0,\varpi) = 0. \quad (8)$$

Applying the Sh-T of Eq. (8), and making some calculations as a result, we get the following:

$$S[\Xi(v,\varpi)] = \frac{\eta}{\mu}\varpi - \left(\frac{\eta}{\mu}\right)^\varsigma S\left[\frac{\partial^2}{\partial\varpi^2}\Xi(v,\varpi)\right] +$$
$$\left(\frac{\eta}{\mu}\right)^\varsigma S[\Xi(v,\varpi)], \quad (9)$$

Taking the inverse Sh-T on Eq. (9), we have

$$\Xi(v,\varpi) = S^{-1}\left[\frac{\eta}{\mu}\varpi\right] - S^{-1}[\left(\frac{\eta}{\mu}\right)^\varsigma S[\frac{\partial^2}{\partial\varpi^2}\Xi(v,\varpi)]] +$$
$$S^{-1}[\left(\frac{\eta}{\mu}\right)^\varsigma S[\Xi(v,\varpi)]]. \quad (10)$$

Implementing ADM in Eq. (10), therefore, supposes that the solution of Eq. (7) can be expressed as follows:

$$\Xi(v,\varpi) = \sum_{\kappa=0}^{\infty}\Xi_\kappa(v,\varpi). \quad (11)$$

Using Eq. (11) in Eq. (10).

$$\sum_{\kappa=0}^{\infty}\Xi_\kappa(v,\varpi) = S^{-1}\left[\frac{\eta}{\mu}(\varpi)\right] -$$
$$S^{-1}[\left(\frac{\eta}{\mu}\right)^\varsigma S[\frac{\partial^2}{\partial\varpi^2}\sum_{\kappa=0}^{\infty}\Xi_\kappa(v,\varpi)]] +$$
$$S^{-1}[\left(\frac{\eta}{\mu}\right)^\varsigma S[\sum_{\kappa=0}^{\infty}\Xi_\kappa(v,\varpi)]].$$

We obtain the following terms for the series solution by using the method described in the preceding section:

$$\Xi_0(v,\varpi) = S^{-1}[\frac{\eta}{\mu}\varpi],$$

$$\Xi_0(v,\varpi) = \varpi.$$

$$\Xi_1(v,\varpi) = \varpi\frac{v^\varsigma}{\Gamma(\varsigma+1)}.$$

$$\Xi_2(v,\varpi) = \varpi\frac{v^{2\varsigma}}{\Gamma(2\varsigma+1)}.$$

$$\Xi_3(v,\varpi) = \varpi\frac{v^{3\varsigma}}{\Gamma(3\varsigma+1)}.$$

$$\Xi_4(v,\varpi) = \varpi\frac{v^{4\varsigma}}{\Gamma(4\varsigma+1)}.$$

$$\Xi_5(v,\varpi) = \varpi\frac{v^{5\varsigma}}{\Gamma(5\varsigma+1)}.$$

The series forms a solution to the given problem, and we have

$$\Xi(v,\varpi) = \varpi + \varpi\frac{v^\varsigma}{\Gamma(\varsigma+1)} + \varpi\frac{v^{2\varsigma}}{\Gamma(2\varsigma+1)} + \varpi\frac{v^{3\varsigma}}{\Gamma(3\varsigma+1)} +$$
$$\varpi\frac{v^{4\varsigma}}{\Gamma(4\varsigma+1)} + \varpi\frac{v^{5\varsigma}}{\Gamma(5\varsigma+1)} + \cdots.$$

$$\Xi(v,\varpi) = \varpi\left(1 + \frac{v^\varsigma}{\Gamma(\varsigma+1)} + \frac{v^{2\varsigma}}{\Gamma(2\varsigma+1)} + \frac{v^{3\varsigma}}{\Gamma(3\varsigma+1)} + \frac{v^{4\varsigma}}{\Gamma(4\varsigma+1)} + \frac{v^{5\varsigma}}{\Gamma(5\varsigma+1)} + \cdots\right).$$

$$\Xi(v,\varpi) = \varpi\sum_{\kappa=0}^{\infty}\frac{v^{\kappa\varsigma}}{\Gamma(\kappa\varsigma+1)}.$$

Using the M-L function, we may establish the Ex-S to Eq. (7) with respect to I-Cs.

$$\Xi(v,\varpi) = \varpi E_\varsigma(v^\varsigma),$$

such that, where $E_\varsigma(v^\varsigma)$ is the M-L function. If $\varsigma = 2$, then

$$E_2(v^2) = \sum_{k=0}^{\infty}\frac{v^{2k}}{\Gamma(2k+1)} = \sum_{k=0}^{\infty}\frac{v^{2k}}{(2k)!} = \cosh v.$$

The Ex-S to Example 1 when $\varsigma = 2$ is $\Xi(v,\varpi) = \varpi\cosh v$. Similarly, STDM can be used to derive the ϖ-space solution as

Adnan Khan, Muhammad Imran Liaqat, Asma Mushtaq
Analytical Analysis for Space Fractional Helmholtz Equations by using the Hybrid Efficient Approach

DOI 10.2478/ama-2024-0065

$$\mathfrak{I}_\varpi^\varsigma \Xi(\nu,\varpi) + \frac{\partial^2}{\partial \nu^2}\Xi(\nu,\varpi) - \Xi(\nu,\varpi) = 0, 1<\varsigma \le 2, \qquad (12)$$

with the I-Cs:

$$\Xi(\nu,0) = \nu, \Xi_\varpi(\nu,0) = 0. \qquad (13)$$

Thus, the series-form solution of Eq. (12) is obtained.

$$\Xi(\nu,\varpi) = \nu \left(1 + \frac{\varpi^\varsigma}{\Gamma(\varsigma+1)} + \frac{\varpi^{2\varsigma}}{\Gamma(2\varsigma+1)} + \frac{\varpi^{3\varsigma}}{\Gamma(3\varsigma+1)} + \frac{\varpi^{4\varsigma}}{\Gamma(4\varsigma+1)} + \frac{\varpi^{5\varsigma}}{\Gamma(5\varsigma+1)} + \cdots \right).$$

In the case when $\varsigma = 2$, then the solution through STDM is $\Xi(\nu,\varpi) = \nu \cosh \varpi$.

Example 2. Consider the ν-space fractional-order HH-E.

$$\mathfrak{I}_\nu^\varsigma \Xi(\nu,\varpi) + \frac{\partial^2}{\partial \varpi^2}\Xi(\nu,\varpi) + 5\Xi(\nu,\varpi,\lambda) = 0, \qquad (14)$$

with the I-Cs

$$\Xi(0,\varpi) = \varpi, \Xi_\nu(0,\varpi) = 0. \qquad (15)$$

Applying the Sh-T of Eq. (14), and making some calculations as a result, we get the following:

$$S[\Xi(\nu,\varpi)] = \frac{\eta}{\mu}\varpi - \left(\frac{\eta}{\mu}\right)^\varsigma S[\frac{\partial^2}{\partial \varpi^2}\Xi(\nu,\varpi)] - 5\left(\frac{\eta}{\mu}\right)^\varsigma S[\Xi(\nu,\varpi)], \qquad (16)$$

Taking the inverse Sh-T on Eq. (16), we have

$$\Xi(\nu,\varpi) = S^{-1}[\frac{\eta}{\mu}\varpi] - S^{-1}[\left(\frac{\eta}{\mu}\right)^\varsigma S[\frac{\partial^2}{\partial \varpi^2}\Xi(\nu,\varpi)]] - 5S^{-1}[\left(\frac{\eta}{\mu}\right)^\varsigma S[\Xi(\nu,\varpi)]]. \qquad (17)$$

Implementing ADM in Eq. (17), therefore, supposes that the solution of Eq. (14) can be represented in the following form:

$$\Xi(\nu,\varpi) = \sum_{\kappa=0}^\infty \Xi_\kappa(\nu,\varpi). \qquad (18)$$

$$\sum_{\kappa=0}^\infty \Xi_\kappa(\nu,\varpi) = S^{-1}[\frac{\eta}{\mu}\varpi] - S^{-1}[\left(\frac{\eta}{\mu}\right)^\varsigma S[\frac{\partial^2}{\partial \varpi^2}\sum_{\kappa=0}^\infty \Xi_\kappa(\nu,\varpi)]] - 5S^{-1}[\left(\frac{\eta}{\mu}\right)^\varsigma S[\sum_{\kappa=0}^\infty \Xi_\kappa(\nu,\varpi)]].$$

By using the procedure as explained in the previous section, we get the following terms for the series solution:

$$\Xi_0(\nu,\varpi) = S^{-1}\left[\frac{\eta}{\mu}(\varpi)\right],$$

$$\Xi_0(\nu,\varpi) = \varpi.$$

$$\Xi_1(\nu,\varpi) = (-5)\varpi \frac{\nu^\varsigma}{\Gamma(\varsigma+1)}.$$

$$\Xi_2(\nu,\varpi) = (-5)^2\varpi \frac{\nu^{2\varsigma}}{\Gamma(2\varsigma+1)}.$$

$$\Xi_3(\nu,\varpi) = (-5)^3\varpi \frac{\nu^{3\varsigma}}{\Gamma(3\varsigma+1)}.$$

$$\Xi_4(\nu,\varpi) = (-5)^4\varpi \frac{\nu^{4\varsigma}}{\Gamma(4\varsigma+1)}.$$

$$\Xi_5(\nu,\varpi) = (-5)^5(\varpi + \lambda) \frac{\nu^{5\varsigma}}{\Gamma(5\varsigma+1)}.$$

The series forms a solution to the given problem, and we have

$$\Xi(\nu,\varpi) = \varpi + (-5)\varpi \frac{\nu^\varsigma}{\Gamma(\varsigma+1)} + (-5)^2\varpi \frac{\nu^{2\varsigma}}{\Gamma(2\varsigma+1)} + (-5)^2\varpi \frac{\nu^{3\varsigma}}{\Gamma(3\varsigma+1)} + (-5)^2\varpi \frac{\nu^{4\varsigma}}{\Gamma(4\varsigma+1)} + (-5)^2\varpi \frac{\nu^{5\varsigma}}{\Gamma(5\varsigma+1)} + \cdots .$$

$$\Xi(\nu,\varpi) = \varpi \left(1 + \frac{(-5\nu^\varsigma)}{\Gamma(\varsigma+1)} + \frac{(-5\nu^\varsigma)^2}{\Gamma(2\varsigma+1)} + \frac{(-5\nu^\varsigma)^3}{\Gamma(3\varsigma+1)} + \frac{(-5\nu^\varsigma)^4}{\Gamma(4\varsigma+1)} + \frac{(-5\nu^\varsigma)^5}{\Gamma(5\varsigma+1)} + \cdots \right).$$

We can determine the Ex-S to Eq. (14) with respect to I-Cs by using the ML-F

$$\Xi(\nu,\varpi) = \varpi E_\varsigma(-5\nu^\varsigma).$$

If $\varsigma = 2$, then

$$E_2(-5\nu^2) = \sum_{k=0}^\infty \frac{(-5\nu^2)^k}{\Gamma(2k+1)} = \sum_{k=0}^\infty \frac{(-1)^k(\sqrt{5}\nu)^{2k}}{\Gamma(2k+1)} = \sum_{k=0}^\infty \frac{(-1)^k(\sqrt{5}\nu)^{2k}}{(2k)!} = \cosh \sqrt{5}\,\nu.$$

The Ex-S to Example 2 when $\varsigma = 2$ is $\Xi(\nu,\varpi) = \varpi \cosh \sqrt{5}\,\nu$. Similarly, STDM can be used to derive the ϖ-space solution as

$$\mathfrak{I}_\varpi^\varsigma \Xi(\nu,\varpi) + \frac{\partial^2}{\partial \nu^2}\Xi(\nu,\varpi) + 5\Xi(\nu,\varpi,\lambda) = 0, \qquad (19)$$

with the I-Cs

$$\Xi(\nu,0) = \nu, \Xi_\varpi(\nu,0) = 0. \qquad (20)$$

Thus, the series-form solution of Eq. (19) is obtained.

$$\Xi(\nu,\varpi) = \nu \left(1 + \frac{(-5\varpi^\varsigma)}{\Gamma(\varsigma+1)} + \frac{(-5\varpi^\varsigma)^2}{\Gamma(2\varsigma+1)} + \frac{(-5\varpi^\varsigma)^3}{\Gamma(3\varsigma+1)} + \frac{(-5\varpi^\varsigma)^4}{\Gamma(4\varsigma+1)} + \frac{(-5\varpi^\varsigma)^5}{\Gamma(5\varsigma+1)} + \cdots \right).$$

In the case when $\varsigma = 2$, then the solution through STDM is $\Xi(\nu,\varpi) = \nu \cosh \sqrt{5}\,\varpi$.

Example 3. Consider the ν-space fractional-order HH-E.

$$\mathfrak{I}_\nu^\varsigma \Xi(\nu,\varpi) + \frac{\partial^2}{\partial \varpi^2}\Xi(\nu,\varpi) - 2\Xi(\nu,\varpi,\lambda) = (12\nu^2 - 3\nu^4) \sin \varpi, 1<\varsigma \le 2, 0<\varpi \le 2\pi, \qquad (21)$$

with the I-Cs

$$\Xi(0,\varpi) = 0, \Xi_\nu(0,\varpi) = 0. \qquad (22)$$

Applying the Sh-T to Eq. (21), we use the differentiation property of the Sh-T, and after some calculation, as a result, we get as follows:

$$S[\Xi(\nu,\varpi)] = -\left(\frac{\eta}{\mu}\right)^\varsigma S[\frac{\partial^2}{\partial \varpi^2}\Xi(\nu,\varpi)] + 2\left(\frac{\eta}{\mu}\right)^\varsigma S[\Xi(\nu,\varpi)] + \left(\frac{\eta}{\mu}\right)^\varsigma \left(12 \times 2! \left(\frac{\mu}{\eta}\right)^3 - 3 \times 4! \left(\frac{\mu}{\eta}\right)^4\right) \sin \varpi. \qquad (23)$$

Taking the inverse Sh-T on Eq. (23), we have

$$\Xi(\nu,\varpi) = S^{-1}[-\left(\frac{\eta}{\mu}\right)^\varsigma S[\frac{\partial^2}{\partial \varpi^2}\Xi(\nu,\varpi)]$$
$$+ S^{-1}[2\left(\frac{\eta}{\mu}\right)^\varsigma S[\Xi(\nu,\varpi)]$$
$$+ S^{-1}[\left(\frac{\eta}{\mu}\right)^\varsigma \left(12 \times 2! \left(\frac{\mu}{\eta}\right)^3 - 3 \times 4! \left(\frac{\mu}{\eta}\right)^4\right) \sin \varpi]. \qquad (24)$$

Implementing ADM in Eq. (24), therefore, supposes that the solution of Eq. (21) can be represented in the following form:

$$\Xi(\nu,\varpi) = \sum_{\kappa=0}^{\infty} \Xi_\kappa(\nu,\varpi). \tag{25}$$

$$\sum_{\kappa=0}^{\infty} \Xi_\kappa(\nu,\varpi) = S^{-1}[-\left(\frac{\eta}{\mu}\right)^\varsigma S[\frac{\partial^2}{\partial \varpi^2} \sum_{\kappa=0}^{\infty} \Xi_\kappa(\nu,\varpi)]]$$

$$+S^{-1}[2\left(\frac{\eta}{\mu}\right)^\varsigma S[\sum_{\kappa=0}^{\infty} \Xi_\kappa(\nu,\varpi)]] +$$

$$S^{-1}[\left(\frac{\eta}{\mu}\right)^\varsigma (12 \times 2! \left(\frac{\mu}{\eta}\right)^3 - 3 \times 4! \left(\frac{\mu}{\eta}\right)^4) \sin \varpi]. \tag{26}$$

By using the procedure as explained in the previous section, we get the following terms for the series solution:

$$\Xi_0(\nu,\varpi) = S^{-1}[\left(\frac{\eta}{\mu}\right)^\varsigma (12 \times 2! \left(\frac{\mu}{\eta}\right)^3 - 3 \times 4! \left(\frac{\mu}{\eta}\right)^4) \sin \varpi],$$

$$\Xi_0(\nu,\varpi) = (12\nu^2 - 3\nu^4) \sin \varpi.$$

$$\Xi_1(\nu,\varpi) = S^{-1}[-\left(\frac{\eta}{\mu}\right)^\varsigma S[\frac{\partial^2}{\partial \varpi^2} \Xi_0(\nu,\varpi)]] +$$

$$S^{-1}[2\left(\frac{\eta}{\mu}\right)^\varsigma S[\Xi_0(\nu,\varpi)]],$$

$$\Xi_1(\nu,\varpi) = \left(72\frac{\nu^{\varsigma+2}}{\Gamma(\varsigma+2)} - \frac{216\nu^{\varsigma+4}}{\Gamma(\varsigma+4)}\right) \sin \varpi.$$

$$\Xi_2(\nu,\varpi) = S^{-1}[-\left(\frac{\eta}{\mu}\right)^\varsigma S[\frac{\partial^2}{\partial \varpi^2} \Xi_1(\nu,\varpi)]] +$$

$$S^{-1}[2\left(\frac{\eta}{\mu}\right)^\varsigma S[\Xi_1(\nu,\varpi)]].$$

$$\Xi_2(\nu,\varpi) = \left(\frac{216\nu^{2\varsigma+2}}{\Gamma(2\varsigma+2)} - \frac{648\nu^{2\varsigma+4}}{\Gamma(2\varsigma+4)}\right) \sin \varpi.$$

$$\Xi_3(\nu,\varpi) = \left(\frac{648\nu^{3\varsigma+2}}{\Gamma(3\varsigma+2)} - \frac{1944\nu^{3\varsigma+4}}{\Gamma(3\varsigma+4)}\right) \sin \varpi.$$

$$\Xi_4(\nu,\varpi) = \left(\frac{1944\nu^{4\varsigma+2}}{\Gamma(4\varsigma+2)} - \frac{5842\nu^{4\varsigma+4}}{\Gamma(4\varsigma+4)}\right) \sin \varpi.$$

$$\Xi_5(\nu,\varpi) = \left(\frac{5832\nu^{5\varsigma+2}}{\Gamma(4\varsigma+2)} - \frac{17496\nu^{5\varsigma+4}}{\Gamma(4\varsigma+4)}\right) \sin \varpi.$$

The series forms a solution to the given problem, and we have

$$\Xi(\nu,\varpi) = (12\nu^2 - 3\nu^4) \sin \varpi + \left(\frac{216\nu^{2\varsigma+2}}{\Gamma(2\varsigma+2)} - \frac{648\nu^{2\varsigma+4}}{\Gamma(2\varsigma+4)}\right) \sin \varpi + \left(\frac{648\nu^{3\varsigma+2}}{\Gamma(3\varsigma+2)} - \frac{1944\nu^{3\varsigma+4}}{\Gamma(3\varsigma+4)}\right) \sin \varpi + \left(\frac{1944\nu^{4\varsigma+2}}{\Gamma(4\varsigma+2)} - \frac{5842\nu^{4\varsigma+4}}{\Gamma(4\varsigma+4)}\right) \sin \varpi + \left(\frac{5832\nu^{5\varsigma+2}}{\Gamma(4\varsigma+2)} - \frac{17496\nu^{5\varsigma+4}}{\Gamma(4\varsigma+4)}\right) \sin \varpi \cdots.$$

The Ex-S to Example 3 when $\varsigma = 2$ is $\Xi(\nu,\varpi) = 9\nu^4 \sin \varpi + 12\nu^2 \sin \varpi$. Similarly, STDM can be used to derive the ϖ -space solution as

$$\mathfrak{I}_\varpi^\varsigma \Xi(\nu,\varpi) + \frac{\partial^2}{\partial \nu^2} \Xi(\nu,\varpi) - 2\Xi(\nu,\varpi,\lambda)$$

$$= (12\varpi^2 - 3\varpi^4) \sin \nu, 1<\varsigma \le 2, 0<\nu \le 2\pi,$$

with the I-Cs

$$\Xi(\nu,0) = 0, \Xi_\varpi(\nu,0) = 0.$$

Thus, the series-form solution of ϖ-space problem is obtained.

$$\Xi(\nu,\varpi) = (12\varpi^2 - 3\varpi^4) \sin \nu + \left(\frac{216\varpi^{2\varsigma+2}}{\Gamma(2\varsigma+2)} - \frac{648\varpi^{2\varsigma+4}}{\Gamma(2\varsigma+4)}\right) \sin \nu + \left(\frac{648\varpi^{3\varsigma+2}}{\Gamma(3\varsigma+2)} - \frac{1944\varpi^{3\varsigma+4}}{\Gamma(3\varsigma+4)}\right) \sin \nu + \left(\frac{1944\varpi^{4\varsigma+2}}{\Gamma(4\varsigma+2)} - \frac{5842\varpi^{4\varsigma+4}}{\Gamma(4\varsigma+4)}\right) \sin \nu + \left(\frac{5832\varpi^{5\varsigma+2}}{\Gamma(4\varsigma+2)} - \frac{17496\varpi^{5\varsigma+4}}{\Gamma(4\varsigma+4)}\right) \sin \nu \cdots.$$

In the case when $\varsigma = 2$, then the solution through STDM is $(\nu,\varpi) = 9\varpi^4 \sin \nu + 12\varpi^2 \sin \nu$.

5. GRAPHICAL AND NUMERICAL RESULTS WITH DISCUSSION

In this section, we assess the numerical and graphic outcomes of the App-S and Ex-S to the models discussed in Examples 1, 2, and 3. The precision and efficiency of the approximate approach can be assessed using error functions. An approximate analytical solution is provided by STDM in terms of an infinite fractional power series, and the approximate solution's errors must be specified. Rec-Er, Abs-Er, and Rel-Er functions are the functions that we use to illustrate the precision and efficiency of STDM.

The Abs-Er, Rel-Er, and Rec-Er are defined as follows:

$$\Xi(\nu,\varpi) \approx \Xi^\kappa(\nu,\varpi), \kappa = 1,2,3,\ldots..$$

where, $\Xi^\kappa(\nu,\varpi)$ and $\Xi(\nu,\varpi)$ are the κth-step App-S and Ex-S respectively.

The Abs-Er for the κth-step App-S is calculated as

$$\text{Abs. Er}^\kappa = |\Xi(\nu,\varpi) - \Xi^\kappa(\nu,\varpi)|.$$

The Rel-Er for the κth-step App-S is calculated as

$$\text{Rel. Er}^\kappa = \frac{|\Xi(\nu,\varpi) - \Xi^\kappa(\nu,\varpi)|}{|\Xi(\nu,\varpi)|}.$$

The Rec-Er for the κth-step App-S is calculated as

$$\text{Rec. Error}^\kappa = |\Xi^{\kappa+1}(\nu,\varpi) - \Xi^\kappa(\nu,\varpi)|.$$

The two-dimensional graphs of the App-S acquired from five iterations and the Ex-S derived by STDM for $\varsigma = 1.6, 1.7, 1.8, 1.9$ and 2 are shown in Figures 1 of Examples 1–3. These graphs show how, when $\zeta \to 2$ occurs, the App-S converges to the Ex-S. The App-S interaction with the Ex-S when $\zeta = 2$ occurs demonstrates the accuracy of the proposed approach.

The Abs-E and Rel-E in the interval $\nu \epsilon [0,1]$ between the Ex-S and fifth-order App-S derived by STDM in Problems 1–3 at $\varsigma = 2$ are shown in graphs 2 and 3 respectively. The graphs demonstrate that the App-S and Ex-S are almost in agreement, which attests to the STDM's efficiency.

Tables 1–3 display Abs-Er at reasonable nominated grid points in the interval $\upsilon \in [0, 1]$ amongst the 5th-step App-S and Ex-S attained using STDM of Examples 1, 2, and 3 at $\varsigma = 1.6, 1.7, 1.8, 1.9$ and 2. From Tables 1–3, we observe that the Abs-Er for test examples for all FOD is very small. If we increase the order of the FOD of the 5th-step App-S, the Abs-Er further decreases.

The convergence of the App-S to the Ex-S for Examples 1, 2, and 3 is shown numerically with the help of Rec-Er at reasonable nominated grid points in the interval $\nu \in [0,1]$, as shown in Tables 4–9. We see from Tables 4–9 that, on increasing the order of the FOD, the 5th-step App-S obtained by the proposed approach

Adnan Khan, Muhammad Imran Liaqat, Asma Mushtaq
Analytical Analysis for Space Fractional Helmholtz Equations by using the Hybrid Efficient Approach

DOI 10.2478/ama-2024-0065

converges rapidly to the Ex-S. We can see from Tables 4–6 that there is a very minor Abs-Er for all of the test problems for 4th-step App-S. We see from Tables 7–9 that, considering the 5th-step App-S results in an even smaller Rec-Er, since our suggested approach is accurate, as seen by this process of Rec-Er, the App-S is rapidly approaching the Ex-S. Thus, we deduce that the suggested approach is a useful and efficient approach for solving FODE with a reduced number of computations and iteration steps.

The graphs and tables show that the App-S and Ex-S agree, confirming the effectiveness of the recommended approach. Therefore, based on Figures 1-3 and Tables 1–9, we deduce that STDM provides us with a solution in a fractional power series that has a small error.

The following are the 2D graphs showing the $\Xi(\nu, \varpi)$ and $\Xi^5(\nu, \varpi)$ at $\varsigma = 1.6, 1.7, 1.8, 1.9$ and 2 in the interval $\nu \in [0, 1]$ for Examples 1, 2, and 3.

(a)

(b)

(c)
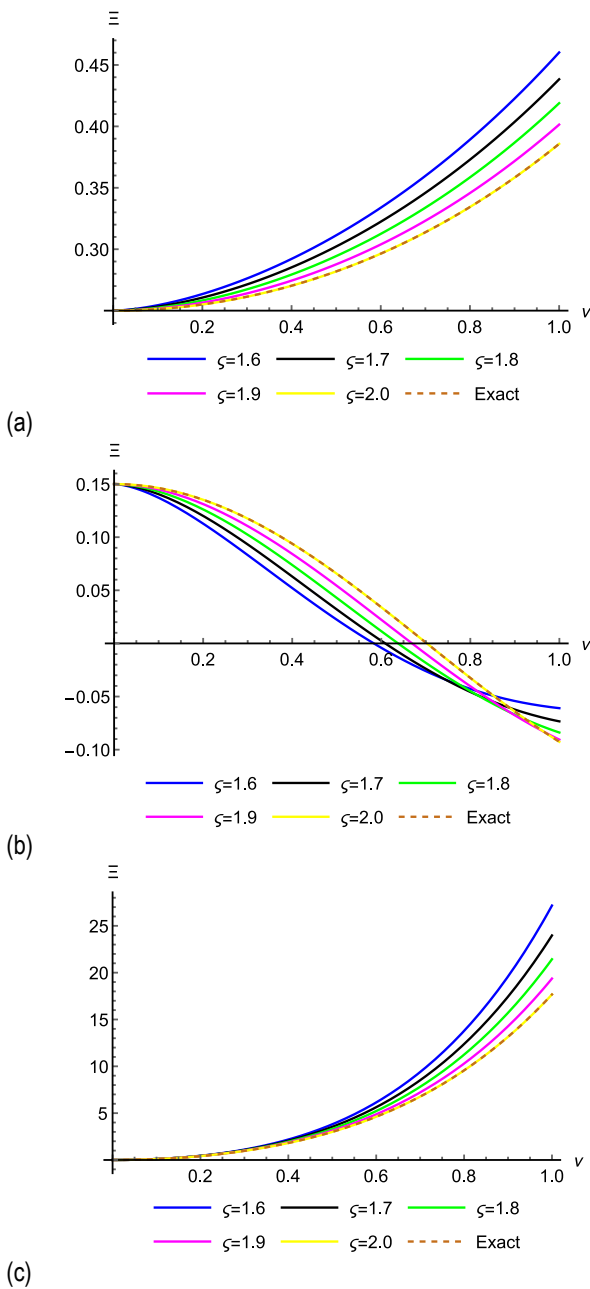
Fig. 1. The 5th-step App-S and Ex-S at $\varsigma = 1.6, 1.7, 1.8, 1.9,$ and 2 for Example 1, 2 and 3. (a): Example 1 when $\varpi = 0.25$, (b): Example 2 when $\varpi = 0.15$, (c): Example 3 $\varpi = 1$.

The following are the 2D graphs showing the Abs-Er of $\Xi(\nu, \varpi)$ and $\Xi^5(\nu, \varpi)$ at $\varsigma = 2$ in the interval $\nu \in [0, 1]$ for Examples 1, 2, and 3.

(a)

(b)

(c)
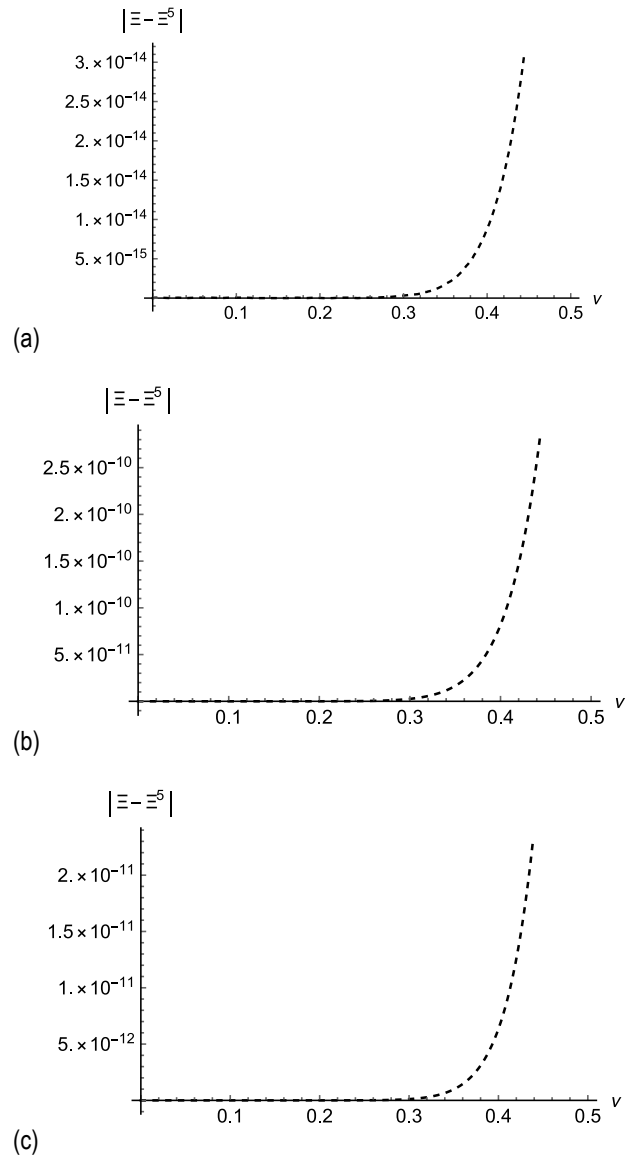
Fig. 2: The Abs-Er of Examples 1, 2, and 3. (a): Example 1 when $\varpi = 0.25$, (b): Example 2 when $\varpi = 0.15$, (c): Example 3 $\varpi = 1$.

The following are the 2D graphs showing the Rel-Er of $\Xi(\nu, \varpi)$ and $\Xi^5(\nu, \varpi)$ at $\varsigma = 2$ in the interval $\nu \in [0, 1]$ for Examples 1, 2, and 3.
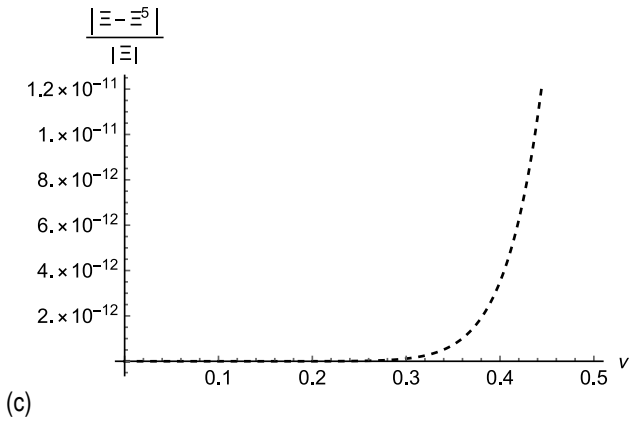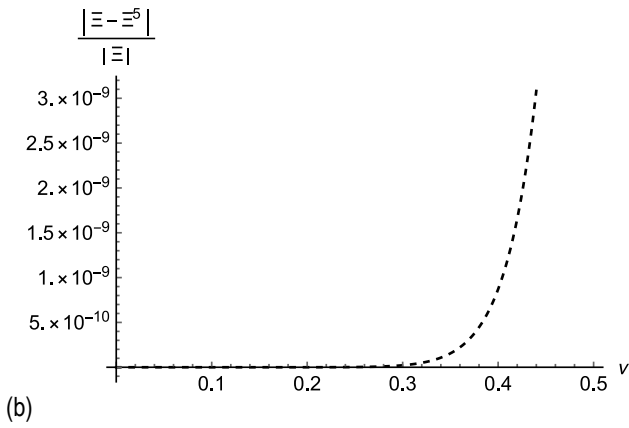

(a)

(b)

(c)
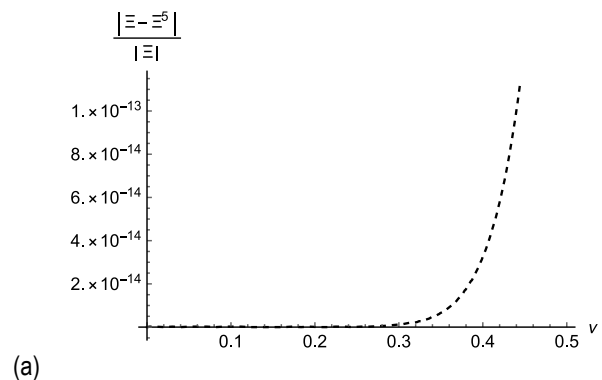
Fig. 3. The Rel-Er of Examples 1, 2, and 3. (a): Example 1 when $\varpi = 0.25$, (b): Example 2 when $\varpi = 0.15$, (c): Example 3 $\varpi = 1$

Tab. 1. The Abs-Er for $\Xi^5(\nu, \varpi)$ when $\varpi = 0.25$ in Example 1 for $\varsigma = 1.7, 1.8, 1.9$ and 2.0

ν	$\varsigma = 1.7$	$\varsigma = 1.8$	$\varsigma = 1.9$	$\varsigma = 2.0$
0.1	0.00198	0.00111	0.00047	0
0.2	0.00557	0.00327	0.00144	0
0.3	0.00998	0.00598	0.00269	2.775×10^{-16}
0.4	0.01493	0.00908	0.00415	8.715×10^{-15}
0.5	0.02029	0.01248	0.00576	1.275×10^{-13}
0.6	0.02602	0.01612	0.00751	1.138×10^{-12}
0.7	0.03209	0.020007	0.00937	7.243×10^{-12}
0.8	0.03852	0.02411	0.01135	3.599×10^{-11}
0.9	0.04533	0.02847	0.01344	1.480×10^{-10}
1.0	0.05257	0.03310	0.01567	5.247×10^{-10}

Tab. 2. The Abs-Er for $\Xi^5(\nu, \varpi)$ when $\varpi = 0.15$ in Example 2 for $\varsigma = 1.7, 1.8, 1.9$ and 2.0

ν	$\varsigma = 1.7$	$\varsigma = 1.8$	$\varsigma = 1.9$	$\varsigma = 2.0$
0.1	0.00580	0.00328	0.00139	0
0.2	0.01520	0.00909	0.00407	$2.00117700 \times 10^{-14}$
0.3	0.02431	0.01516	0.00704	$2.59392507 \times 10^{-12}$
0.4	0.03092	0.02005	0.00964	$8.17310941 \times 10^{-11}$
0.5	0.03361	0.02273	0.01134	1.1864156×10^{-9}
0.6	0.03158	0.02252	0.01175	1.0546420×10^{-8}
0.7	0.02466	0.01909	0.01062	6.6822825×10^{-8}
0.8	0.01324	0.01244	0.00788	$3.30409738 \times 10^{-7}$
0.9	0.00182	0.00295	0.00357	0.000001351
1.0	0.01922	0.00872	0.002042	0.0000047612

Tab. 3. The Abs-Er for $\Xi^5(\nu, \varpi)$ when $\varpi = 1$ in Example 3 for $\varsigma = 1.7, 1.8, 1.9$ and 2.0

ν	$\varsigma = 1.7$	$\varsigma = 1.8$	$\varsigma = 1.9$	$\varsigma = 2.0$
0.1	4.4×10^{-3}	4.3×10^{-3}	4.1×10^{-4}	0
0.2	4.5×10^{-3}	4.4×10^{-3}	4.0×10^{-4}	0
0.3	4.6×10^{-3}	4.5×10^{-3}	7.0×10^{-4}	1.5×10^{-17}
0.4	4.7×10^{-3}	4.6×10^{-3}	9.6×10^{-4}	1.71×10^{-16}
0.5	4.8×10^{-3}	4.7×10^{-3}	1.1×10^{-4}	1.98×10^{-15}
0.6	4.9×10^{-3}	4.8×10^{-3}	1.1×10^{-4}	2.05×10^{-14}
0.7	5.0×10^{-3}	4.9×10^{-3}	1.0×10^{-4}	2.08×10^{-13}
0.8	5.1×10^{-3}	5.0×10^{-3}	7.8×10^{-4}	2.09×10^{-11}
0.9	5.2×10^{-3}	5.1×10^{-3}	3.5×10^{-4}	2.31×10^{-11}
1.0	5.3×10^{-3}	5.2×10^{-3}	2.0×10^{-4}	2.39×10^{-11}

Tab. 4. The Rec-Er for $\Xi^4(\nu, \varpi)$ when $\varpi = 0.25$ for $\varsigma = 1.7, 1.8, 1.9$ and 2.0 for Example 1

ν	$\varsigma = 1.7$	$\varsigma = 1.8$	$\varsigma = 1.9$	$\varsigma = 2.0$
0.1	1.17×10^{-11}	2.0×10^{-12}	3.6×10^{-13}	6.2×10^{-14}
0.2	1.3×10^{-9}	3.0×10^{-10}	7.0×10^{-11}	1.5×10^{-11}
0.3	2.0×10^{-8}	5.6×10^{-9}	1.5×10^{-9}	4.0×10^{-10}
0.4	1.4×10^{-7}	4.5×10^{-8}	1.3×10^{-8}	4.0×10^{-9}
0.5	3.0×10^{-8}	2.2×10^{-7}	7.4×10^{-8}	2.4×10^{-8}
0.6	6.4×10^{-9}	8.3×10^{-7}	2.9×10^{-7}	1.0×10^{-7}
0.7	6.5×10^{-6}	2.5×10^{-6}	9.6×10^{-7}	3.5×10^{-7}
0.8	1.6×10^{-5}	6.6×10^{-6}	2.6×10^{-6}	1.0×10^{-6}
0.9	3.6×10^{-5}	1.5×10^{-5}	6.4×10^{-6}	2.6×10^{-6}
10	7.4×10^{-5}	3.3×10^{-5}	1.4×10^{-5}	6.2×10^{-6}

Tab. 5. The Rec-Er for $\Xi^4(\nu, \varpi)$ when $\varpi = 0.15$ for $\varsigma = 1.7, 1.8, 1.9$ and 2.0 for Example 2

ν	$\varsigma = 1.7$	$\varsigma = 1.8$	$\varsigma = 1.9$	$\varsigma = 2.0$
0.1	4.3×10^{-9}	7.8×10^{-10}	1.3×10^{-10}	2.3×10^{-11}
0.2	4.9×10^{-7}	1.1×10^{-7}	2.6×10^{-8}	5.9×10^{-9}
0.3	7.7×10^{-6}	2.1×10^{-6}	5.7×10^{-7}	1.5×10^{-7}
0.4	5.4×10^{-5}	1.6×10^{-5}	5.1×10^{-6}	1.5×10^{-6}
0.5	2.4×10^{-4}	8.4×10^{-5}	2.7×10^{-6}	9.0×10^{-6}
0.6	8.6×10^{-4}	3.1×10^{-4}	1.1×10^{-4}	3.9×10^{-5}
0.7	2.4×10^{-3}	9.5×10^{-4}	3.6×10^{-4}	1.3×10^{-4}
0.8	6.0×10^{-3}	2.4×10^{-3}	9.9×10^{-4}	3.9×10^{-4}
0.9	1.3×10^{-2}	5.8×10^{-3}	2.4×10^{-3}	1.0×10^{-3}
10	2.7×10^{-2}	1.2×10^{-2}	5.4×10^{-3}	2.3×10^{-3}

Tab. 6. The Rec-Er for $\Xi^4(\nu, \varpi)$ when $\varpi = 1$ for $\varsigma = 1.7, 1.8, 1.9$ and 2.0 for Example 3

ν	$\varsigma = 1.7$	$\varsigma = 1.8$	$\varsigma = 1.9$	$\varsigma = 2.0$
0.1	9.8×10^{-11}	1.6×10^{-11}	2.7×10^{-12}	4.5×10^{-13}
0.2	4.3×10^{-8}	9.7×10^{-9}	2.1×10^{-9}	4.6×10^{-10}
0.3	1.5×10^{-6}	4.0×10^{-7}	1.0×10^{-7}	2.6×10^{-8}
0.4	1.9×10^{-5}	5.7×10^{-6}	1.6×10^{-6}	4.7×10^{-7}
0.5	1.3×10^{-4}	4.4×10^{-5}	1.4×10^{-5}	4.3×10^{-6}
0.6	6.8×10^{-4}	2.3×10^{-4}	8.0×10^{-5}	2.6×10^{-5}
0.7	2.6×10^{-3}	9.7×10^{-4}	3.5×10^{-4}	1.2×10^{-4}
0.8	8.5×10^{-3}	3.3×10^{-3}	1.2×10^{-3}	4.7×10^{-4}
0.9	2.3×10^{-2}	9.7×10^{-3}	3.9×10^{-3}	1.5×10^{-3}
10	5.9×10^{-2}	2.5×10^{-2}	1.0×10^{-2}	9.0×10^{-2}

Adnan Khan, Muhammad Imran Liaqat, Asma Mushtaq
Analytical Analysis for Space Fractional Helmholtz Equations by using the Hybrid Efficient Approach

DOI 10.2478/ama-2024-0065

Tab. 7. The Rec-Er for $\Xi^5(\nu, \varpi)$ when $\varpi = 0.25$ for $\varsigma = 1.7, 1.8, 1.9$ and 2.0 for Example 1

ν	$\varsigma = 1.7$	$\varsigma = 1.8$	$\varsigma = 1.9$	$\varsigma = 2.0$
0.1	6.6×10^{-15}	6.8×10^{-16}	6.9×10^{-17}	6.8×10^{-18}
0.2	2.3×10^{-12}	3.5×10^{-13}	5.0×10^{-14}	7.0×10^{-15}
0.3	7.5×10^{-11}	1.3×10^{-11}	2.3×10^{-12}	4.0×10^{-13}
0.4	8.6×10^{-10}	1.8×10^{-10}	3.6×10^{-11}	7.2×10^{-12}
0.5	5.7×10^{-9}	1.3×10^{-9}	3.0×10^{-10}	6.7×10^{-11}
0.6	2.7×10^{-8}	6.9×10^{-9}	1.7×10^{-9}	4.1×10^{-10}
0.7	1.0×10^{-7}	2.7×10^{-8}	7.4×10^{-9}	1.9×10^{-9}
0.8	3.1×10^{-7}	9.2×10^{-8}	2.6×10^{-8}	7.3×10^{-9}
0.9	8.5×10^{-7}	2.6×10^{-7}	8.1×10^{-8}	2.4×10^{-8}
10	2.0×10^{-6}	6.8×10^{-7}	2.2×10^{-7}	6.8×10^{-8}

Tab. 8. The Rec-Er for $\Xi^5(\nu, \varpi)$ when $\varpi = 0.15$ for $\varsigma = 1.7, 1.8, 1.9$ and 2.0 for Example 2

ν	$\varsigma = 1.7$	$\varsigma = 1.8$	$\varsigma = 1.9$	$\varsigma = 2.0$
0.1	1.2×10^{-11}	1.2×10^{-12}	1.3×10^{-13}	1.2×10^{-14}
0.2	4.4×10^{-9}	6.6×10^{-10}	9.4×10^{-11}	1.3×10^{-11}
0.3	1.4×10^{-7}	2.5×10^{-8}	4.4×10^{-9}	7.6×10^{-10}
0.4	1.6×10^{-6}	3.3×10^{-7}	6.8×10^{-8}	1.3×10^{-8}
0.5	1.0×10^{-5}	2.5×10^{-6}	5.7×10^{-7}	1.2×10^{-7}
0.6	5.1×10^{-5}	1.3×10^{-5}	3.2×10^{-7}	7.8×10^{-7}
0.7	1.8×10^{-4}	5.2×10^{-5}	1.3×10^{-5}	3.6×10^{-6}
0.8	5.8×10^{-4}	1.7×10^{-4}	4.9×10^{-5}	1.3×10^{-5}
0.9	1.6×10^{-3}	5.0×10^{-4}	1.5×10^{-4}	4.5×10^{-5}
10	3.9×10^{-3}	1.2×10^{-3}	4.1×10^{-4}	1.2×10^{-4}

Ta. 9. The Rec-Er for $\Xi^5(\nu, \varpi)$ when $\varpi = 1$ for $\varsigma = 1.7, 1.8, 1.9$ and 2.0 for Example 3

ν	$\varsigma = 1.7$	$\varsigma = 1.8$	$\varsigma = 1.9$	$\varsigma = 2.0$
0.1	1.3×10^{-13}	1.3×10^{-14}	1.3×10^{-15}	1.2×10^{-16}
0.2	1.9×10^{-10}	2.7×10^{-11}	3.7×10^{-12}	5.0×10^{-13}
0.3	1.3×10^{-8}	2.3×10^{-9}	3.9×10^{-10}	6.5×10^{-11}
0.4	2.8×10^{-7}	$5. \times 10^{-8}$	1.0×10^{-8}	2.0×10^{-9}
0.5	2.9×10^{-6}	6.5×10^{-7}	1.4×10^{-7}	2.9×10^{-8}
0.6	2.0×10^{-5}	4.8×10^{-6}	1.1×10^{-6}	$2. \times 10^{-7}$
0.7	1.0×10^{-4}	2.6×10^{-5}	6.7×10^{-6}	1.6×10^{-6}
0.8	4.0×10^{-4}	1.1×10^{-4}	3.1×10^{-5}	8.3×10^{-6}
0.9	1.4×10^{-3}	4.1×10^{-4}	1.2×10^{-4}	3.4×10^{-5}
10	4.2×10^{-3}	1.3×10^{-3}	4.0×10^{-4}	2.5×10^{-5}

6. CONCLUSION

In order to obtain both approximate and exact solutions for the Helmholtz problems in the sense of space CFD, a coupling approach has been employed in this study. An analysis in the form of absolute, relative, and recurrence errors by graphical and numerically means has been done to illustrate the correctness of our approach. For different values of fractional order derivatives, 2D graphs are also established that show the convergence of the approximate solution to the exact solution. These graphs show how, when $\varsigma \to 2$ occurs, the approximate solution converges to the exact solution. The approximate interaction with the exact solution when $\varsigma = 2$ occurs demonstrates the accuracy and efficacy of the proposed approach.

The STDM distinguishes itself from other approximate analytical methods with the following features: The advantage of this method is that it does not call for any presumptions regarding significant or minor physical factors. Because of this, it circumvents some of the drawbacks of conventional perturbation techniques. In contrast to earlier analytic approximation methods, the STDM may generate expansion solutions for FODEs without the need for perturbation, linearization, or discretization. In light of the outcomes, we concluded that STDM is straightforward to use, precise, and effective. We intend to use the STDM in the future to solve diverse nonlinear fractional models that arise in engineering and biological systems.

REFERENCES

1. Djaouti AM, Khan ZA, Liaqat MI, Al-Quran A. A novel technique for solving the nonlinear fractional-order smoking model. Fractal and Fractional. 2024; 8(5):286.
   https://doi.org/10.3390/fractalfract8050286
2. Liaqat MI, Etemad S, Rezapour S, Park C. A novel analytical Aboodh residual power series method for solving linear and nonlinear time-fractional partial differential equations with variable coefficients. AIMS Mathematics. 2022; 7(9):16917-16948.
   https://doi.org/10.3934/math.2022929
3. Djaouti AM, Khan ZA, Liaqat MI, Al-Quran A. Existence uniqueness and averaging principle of fractional neutral stochastic differential equations in the Lp Space with the framework of the Ψ-Caputo derivative. Mathematics. 2024;12(7): 1-21.
   https://doi.org/10.3390/math12071037
4. Owolabi KM, Hammouch Z. Spatiotemporal patterns in the Belousov–Zhabotinskii reaction systems with Atangana–Baleanu fractional order derivative. Physica A: Statistical Mechanics and its Applications. 2019; 523: 1072-1090.
   https://doi.org/10.1016/j.physa.2019.04.017
5. Djaouti AM, Khan ZA, Liaqat MI, Al-Quran A. A Study of Some Generalized Results of Neutral Stochastic Differential Equations in the Framework of Caputo–Katugampola Fractional Derivatives. Mathematics. 2024;12(11): 1654.
   https://doi.org/10.3390/math12111654
6. Tenreiro Machado JA. The bouncing ball and the Grünwald-Letnikov definition of fractional derivative. Fractional Calculus and Applied Analysis. 2021; 24(4): 1003-1014. https://doi.org/10.1515/fca-2021-0043
7. Ahmad B, Ntouyas SK, Alsaedi A. Fractional order differential systems involving right Caputo and left Riemann–Liouville fractional derivatives with nonlocal coupled conditions. Boundary value problems. 2019(1): 1-12. https://doi.org/10.1186/s13661-019-1222-0
8. Sene N. Analysis of a fractional-order chaotic system in the context of the Caputo fractional derivative via bifurcation and Lyapunov exponents. Journal of King Saud University-Science. 2021; 33(1): 101275. https://doi.org/10.1016/j.jksus.2020.101275
9. Shah K, Alqudah MA, Jarad F, Abdeljawad T. Semi-analytical study of Pine Wilt Disease model with convex rate under Caputo–Febrizio fractional order derivative. Chaos, Solitons&Fractals. 2020;135: 109754. https://doi.org/10.1016/j.chaos.2020.109754
10. Ghanbari B, Djilali S. Mathematical and numerical analysis of a three-species predator-prey model with herd behavior and time fractional-order derivative. Mathematical Methods in the Applied sciences, 2020; 43(4):1736-1752. https://doi.org/10.1002/mma.5999
11. Liaqat MI, Akgül A, Prosviryakov EY. An efficient method for the analytical study of linear and nonlinear time-fractional partial differential equations with variable coefficients. Journal of Samara State Technical University. Ser. Physical and Mathematical Sciences. 2023; 27(2): 214-240. https://doi.org/10.14498/vsgtu2009
12. Liaqat MI, Akgül A, De la Sen M, Bayram, M. Approximate and exact solutions in the sense of conformable derivatives of quantum mechanics models using a novel algorithm. Symmetry. 2023; 15(3): 744. https://doi.org/10.3390/sym15030744

13. Cheng X, Hou J, Wang L. Lie symmetry analysis, invariant subspace method and q-homotopy analysis method for solving fractional system of single-walled carbon nanotube. Computational and Applied Mathematics. 2021; 40:1-17.
https://doi.org/10.1007/s40314-021-01486-7

14. Paliathanasis A, Bogadi RS, Govender M. Lie symmetry approach to the time-dependent Karmarkar condition. The European Physical Journal C. 2022; 82(11): 987. https://doi.org/10.1140/epjc/s10052-022-10929-2

15. Sahoo S, Ray SS, Abdou M.A. New exact solutions for time-fractional Kaup-Kupershmidt equation using improved (G'/G)-expansion and extended (G'/G)-expansion methods. Alexandria Engineering Journal. 2020; 59(5): 3105-3110.
https://doi.org/10.1016/j.cjph.2016.10.019

16. Jena SK, Chakraverty S. Dynamic behavior of an electromagnetic nanobeam using the Haar wavelet method and the higher-order Haar wavelet method. The European Physical Journal Plus. 2019;134(10): 538.
https://doi.org/10.1140/epjp/i2019-12874-8

17. Yi M, Huang J. Wavelet operational matrix method for solving fractional differential equations with variable coefficients. Applied Mathematics and Computation. 2014; 230: 383-394.
https://doi.org/10.1016/j.amc.2013.06.102

18. Cinar M, Secer A, Ozisik M, Bayram M. Derivation of optical solitons of dimensionless Fokas-Lenells equation with perturbation term using Sardar sub-equation method. Optical and Quantum Electronics. 2022; 54(7): 402. https://doi.org/10.1007/s11082-022-03819-0

19. Atabakzadeh MH, Akrami MH, Erjaee GH. Chebyshev operational matrix method for solving multi-order fractional ordinary differential equations. Applied Mathematical Modelling. 2013; 37(20-21): 8903-8911. https://doi.org/10.1016/j.apm.2013.04.019

20. Liaqat MI, Akgül A, Bayram M. Series and closed form solution of Caputo time-fractional wave and heat problems with the variable coefficients by a novel approach. Optical and Quantum Electronics. 2024;56(2):203.
https://doi.org/10.1007/s11082-023-05751-3

21. Naik PA, Zu J, Ghoreishi M. Estimating the approximate analytical solution of HIV viral dynamic model by using homotopy analysis method. Chaos, Solitons & Fractals. 2020;131:109500.
https://doi.org/10.1016/j.chaos.2019.109500Get rights and content

22. Zeidan D, Chau CK, Lu TT, Zheng WQ. Mathematical studies of the solution of Burgers' equations by Adomian decomposition method. Mathematical Methods in the Applied Sciences. 2020; 43(5): 2171-2188. https://doi.org/10.1002/mma.5982

23. Samaniego E, Anitescu C, Goswami S, Nguyen-Thanh VM, Guo H, Hamdia K, Rabczuk T. An energy approach to the solution of partial differential equations in computational mechanics via machine learning: Concepts, implementation and applications. Computer Methods in Applied Mechanics and Engineering. 2020; 362:112790. https://doi.org/10.1016/j.cma.2019.112790

24. Majeed A, Kamran M, Iqbal MK, Baleanu D. Solving time fractional Burgers' and Fisher's equations using cubic B-spline approximation method. Advances in Difference Equations. 2020;(1):1-15. https://doi.org/10.1186/s13662-020-02619-8

25. Ganji RM, Jafari H, Baleanu D. A new approach for solving multi variable orders differential equations with Mittag–Leffler kernel. Chaos. Solitons & Fractals. 2020; 130:109405.
https://doi.org/10.1016/j.chaos.2019.109405

26. Eriqat T, El-Ajou A, Moa'ath NO, Al-Zhour Z, Momani S. A new attractive analytic approach for solutions of linear and nonlinear neutral fractional pantograph equations. Chaos. Solitons&Fractals. 2020; 138: 109957. https://doi.org/10.1016/j.chaos.2020.109957

27. Yüzbaşı Ş. Numerical solutions of fractional Riccati type differential equations by means of the Bernstein polynomials. Applied Mathematics and Computation, 2013;219(11): 6328-6343.
https://doi.org/10.1016/j.amc.2012.12.006

28. Liaqat MI, Akgül A, Abu-Zinadah H. Analytical investigation of some time-fractional Black–Scholes models by the Aboodh residual power series method. Mathematics. 2023;11(2): 276.
https://doi.org/10.3390/math11020276

29. Jafarian A, Mokhtarpour M, Baleanu D. Artificial neural network approach for a class of fractional ordinary differential equation. Neural Computing and Applications. 2017; 28: 765-773.

30. Li HL, Jiang YL, Wang Z, Zhang L, Teng Z. Global Mittag–Leffler stability of coupled system of fractional-order differential equations on network. Applied Mathematics and Computation. 2015;270: 269-277. https://doi.org/10.1016/j.amc.2015.08.043

31. Qureshi S, Kumar P. Using Shehu integral transform to solve fractional order Caputo type initial value problems. Journal of Applied Mathematics and Computational Mechanics. 2019; 18(2):75-83. https://doi.org/10.17512/jamcm.2019.2.07

32. Jena SR, Sahu I. A novel approach for numerical treatment of traveling wave solution of ion acoustic waves as a fractional nonlinear evolution equation on Shehu transform environment. Physica Scripta. 2023; 98(8): 085231.
https://doi.org/10.1088/1402-4896/ace6de

33. Shah R, Saad Alshehry A, Weera W. A semi-analytical method to investigate fractional-order gas dynamics equations by Shehu transform. Symmetry. 2022; 14(7): 1458.
https://doi.org/10.3390/sym14071458

Adnan Khan: https://orcid.org/0000-0002-1490-8576

Muhammad Imran Liaqat: https://orcid.org/0000-0002-5732-9689

Asma Mushtaq: https://orcid.org/0009-0007-3822-114X